RESEARCH ARTICLE

Electrophoretic deposition of cobalt oxide anodes for alkaline membrane water electrolyzer

Alfonso Pozio[1] ⓘ | **Francesco Bozza[1]** | **Nicola Lisi[1]** | **Francesco Mura[2]**

[1]ENEA, C.R. Casaccia, Rome, Italy

[2]Department SBAI, University of Rome "La Sapienza", Rome, Italy

Correspondence
Alfonso Pozio, ENEA, C.R. Casaccia, Via Anguillarese 301, 00123, S. Maria di Galeria (Rome), Italy.
Email: alfonso.pozio@enea.it

Summary

Nanostructured cobalt oxide anodes for alkaline membrane electrolysis cell (AME) were fabricated by electrophoretic deposition (EPD) method directly on AISI-316 sintered metal fiber substrate, and the effect of different amounts of cobalt oxide was evaluated. The influence of the deposition condition on the microstructure and catalytic activity of the anodes was analyzed, showing different characteristics compared to the substrate steel structure. In particular, the catalytic activity for the oxygen evolution reaction (OER) in KOH 0.5 M solution showed an increase depending on the EPD conditions. The composite electrodes were also compared to other materials commonly applied in alkaline electrolysis in order to verify their effective electrocatalytic activity. In particular, the results were compared with electroplated platinum and cobalt with the aim of identifying the better synthesis technique. The results show that the EPD methodology can be adopted to provide an effective method for improving steel anodes of alkaline membrane electrolyzers.

KEYWORDS

cobalt oxide, electrolysis, electrophoresis, OER, stainless steel oxide

1 | INTRODUCTION

The production of hydrogen from renewable source energy (wind, photovoltaic, etc.) represents one of the most interesting ways for long-term energy storage. Water electrolysis is a powerful and efficient method to produce pure hydrogen.[1] Particularly, electrolyzers can be powered by continuous or intermittent systems (renewable sources) increasing effective power-to-gas strategies.[2,3] In this case, the electrolyzer can operate intermittently when renewable energy is available while hydrogen, after a defined compression stage, can be stored in the gas network.[4] However, since hydrogen compression is energetically and economically unfavorable, the production of

hydrogen directly at high pressure is highly desirable. For this purpose, the technology of alkaline electrolyzers is already commercially available; in these devices, non-noble metal catalysts for hydrogen (HER) and oxygen evolution reactions (OER) are applied, both with the possibility of using normal and deionized water.[5,6] However, the maximum pressure obtainable with this type of systems is about 30 bar, a value beyond which the management of the aqueous electrolyte, generally consisting of an alkaline solution, becomes difficult.[7] To overcome this problem and generate hydrogen at higher pressures, a possible solution is represented by anionic membrane electrolyzers, which in theory could allow the hydrogen outlet pressure to rise (Figure 1).
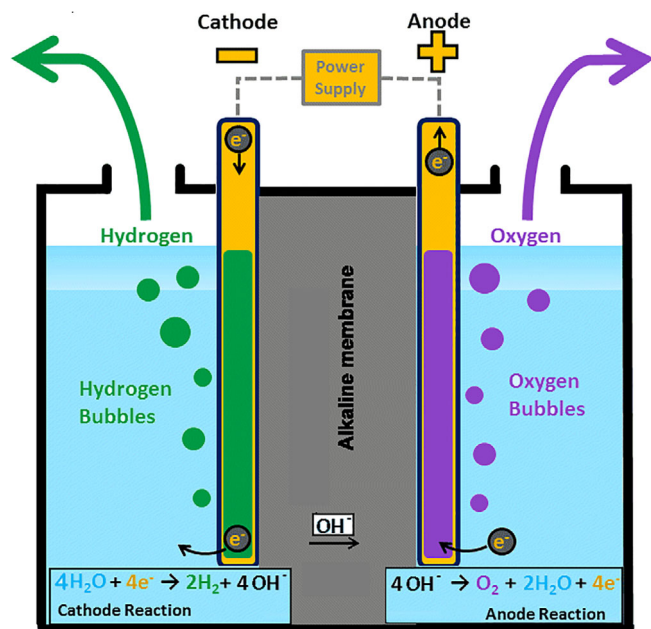
FIGURE 1 Simplified diagram of an electrolysis cell with alkaline membrane

TABLE 1 Medium composition AISI 316 L steel (Bekaert)

%C: 0.024	%Mn: 0.360	%Si: 0.407
%P: 0.018	%S: 0.000	%N: 0.035
%Cr: 6.868	%Ni: 10.056	%Mo 2.532
%Fe: balance		

Alkaline membrane water electrolyzers could offer several other advantages over traditional, liquid electrolyte, alkaline systems including higher energy efficiency, greater hydrogen production rate, and a more compact design,[8,9] all deriving from the presence of the solid-state membrane, in contrast to devices based on free liquid electrolyte and a porous separator.[10] Among the objectives set in the field of research on materials for anionic membrane electrolyzers, the preparation electrodes to interface with the anionic membranes are of primary importance. At present, the preparation of these electrodes is carried out by spray deposition of catalyst powders both on the membranes themselves and on the current carrying supports.[11] The methodology is complex and, in terms of costs and production times, not particularly advantageous. For this reason, other preparation techniques have been investigated such as physical vapor deposition (PVD)[12] or electrodeposition (ED).[13] In this work, we report the results obtained on the application of electrophoretic deposition (EPD) technique for the coating of AME anode substrates with nanosized cobalt oxide powders. In the past, the EPD was already applied for the preparative of nickel oxide electrode for high-rate electrochemical capacitors[14] and for the fabrication of porous anodes solid oxide fuel cells.[15] EPD is a colloidal processing method that allows any substrate that has an electrically conductive surface to be coated with ceramic, metal, or polymeric particles. The EPD process takes place in a deposition bath where particles suspended in a

suitable liquid phase deposit on the surface of the conductive substrate when an electric field applied between the substrate and a counter-electrode.[16,17] EPD technique has the advantage to be low cost, easy to scale up, and widely used technique in industrial applications. It allows to realize coatings with thicknesses with sizes ranging from nm to μm on substrates of complex shape.[18,19] Here, the EPD composite electrodes were compared with electrodes coated with other materials used in this type of cells (nickel, nickel cobalt alloys, Pt, etc.) in order to verify the effective increase in electrocatalytic activity. In particular, the results were compared with those obtained by electroplating (ED) platinum and/or cobalt with the aim of identifying the better synthesis technique. In this study, in particular, we focused on the production of supports coated with cobalt oxide to study the impact of EPD conditions and of the sintering treatment on the catalytic activity of the electrode used as anode in alkaline electrolytic cells. The optimization process took into consideration the morphology of the powders, the thickness of the film, and the optimal sintering treatment that can guarantee the deposited film sufficient mechanical cohesion and without losing excessive surface.

2 | EXPERIMENTAL

2.1 | Materials and electrode preparation

2.1.1 | Substrates

The base material used for the EPD is a commercial matrix of sintered metal fiber made of AISI 316-L (Bekaert) steel, with a thickness of 0.51 mm and a porosity of 82%. This porous substrate is commonly used in filtration processes, but it is also suitable as supports and current conductors in alkaline membrane electrolyzers both at the cathode and at the anode, being chemically stable both in the oxidizing and reducing environment in high pH conditions. The porosity of these structures is a fundamental aspect as it guarantees the passage of the gases that are formed at the membrane/electrode interface and the recirculation of the water/supply solution from any external tanks. Table 1

shows the average composition of the specified steel. As is known, Ni and Fe are considered valid catalysts in alkaline electrolysis.

A small set of different metal substrates were selected to compare with EPD materials from the point of view of their catalytic properties. These are porous matrices of commercial metal fibers without and with ED catalysts.[13]

- A) Ni-Co alloy (72:27%at) (De Nora) (Ni-Co).
- B) Nickel (Bekaert), sintered metal fiber (Ni).
- C) Ni (Bekaert) with electrodeposited Pt (0.75 mg cm^{-2}) (Ni/ED-Pt), D) AISI-316L (Bekaert) with electrodeposited Co (SS/ED-Co) (16.2 mg cm^{-2}).

2.1.2 | Electrophoretic deposition

The process was carried out starting from commercial Co_3O_4 nanopowders (Aldrich, <50 nm). In the EPD process, the powders were first manually ground in an agate mortar, then dispersed, at different concentrations, in a solution of acetyl-acetone, water 10 mL L^{-1}, and metal iodine 2.5 mg L^{-1}, then poured into an electrophoretic cell (Figure 2).

A PTFE electrophoresis cell was made with a volume of 40 mL allowing the coating of substrates from 1 to 8 cm^2. The substrate and the steel counter-electrode are set parallel at a distance of 2 cm, and they are connected respectively to the cathode and anode of a PS251-2 (Aldrich) voltage generator. The cathode of the cell in this case is the substrate, while the anode is an AISI316 sheet. By applying an appropriate electric field, the particles suspended in the positively charged dispersing medium move toward the cathode and are deposited on its surface. The deposition was performed by applying a voltage between 30 and 40 V for a variable amount of time, between 20 and 300 seconds. Afterward, the coated electrode is dried in air and undergoes a heat treatment in air at 600°C for 5 hours to ensure cohesion between the deposited Co_3O_4 particles and to remove solvent residues.

2.2 | Surface analysis

The morphology was investigated by scanning electron microscopy (SEM). All micrographs were acquired with an Auriga Zeiss field emission scanning electron microscope. In order to evaluate the composition of the metal oxide, photoelectron spectroscopy (XPS) measurements of the samples were performed with an ESCALAB MKII spectrometer, equipped with a double anode (Mg, Al) X-ray source, in a 1.0×10^{-9} mbar oil free base vacuum.

2.3 | Electrochemical measurements

Stainless steel (SS) reference material and SS/EPD circular samples (Ø 16 mm) were characterized as anodes in a three-electrode plexiglas (Poly methyl methacrylate) cell and in a small electrolyzer at room temperature.

In the three-electrode cell, the counter-electrode was a platinum sheet (area 10 cm^2), while the reference was a standard calomel electrode (SCE) through a Luggin capillary whose tip was placed as close as possible to the working electrode surface. The cell allows to house the circular sample with an active exposed surface of 0.785 cm^2 in a solution of KOH 0.5 M and positioned in such a way as to be parallel to the counter-electrode at a distance of 1.5 cm.

Potentiodynamic measurements were performed via a potentiostat 1287 (Solartron) at different scan rates between of 1 and 100 mV s^{-1} in the range of potential $-0.24 \div 1.74$ V vs NHE. Galvanostatic polarization curve measurements were also taken with 3 minutes for each current step. Electrochemical impedance spectroscopy (EIS) measurements were also carried out in the frequency range 300 kHz-1 Hz at open circuit potential (OCP). The amplitude of AC signal was always 10 mV$_{pp}$.

To evaluate and compare the performance of the materials, a small 2 cm^2 electrolyzer was used, with porous nickel as a cathode and a commercial anionic membrane (Fumasep FAA-3PK-130) as electrolyte and gas separation system. The cell was (Figure 3) made of
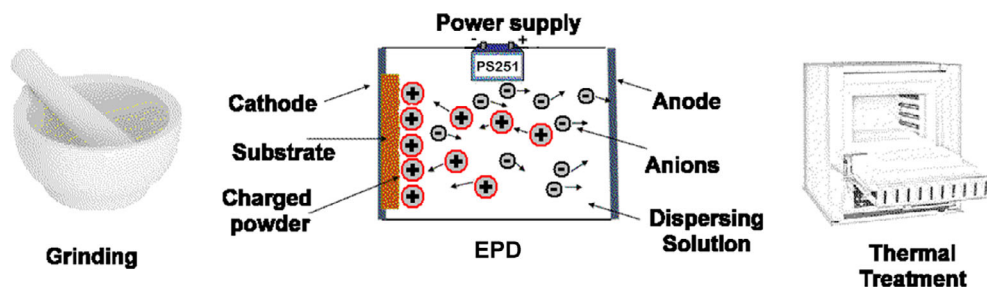

FIGURE 2 Preparation process diagram

FIGURE 3 Electrolysis cell for the characterization of electrodes

steel on both cathode and anodic sides. The anodic side can be fed with distilled water or a KOH solution, contained in a 500 mL polyethylene tank using a metering pump (KMS), in PTFE with a flow of 100 mL min^{-1}. The cathode side output can be connected to a volumetric system for measuring the produced hydrogen.

EIS measurements at OCP and galvanostatic polarization at 200 mA cm^{-2} were carried out. Characteristic curves E vs i were also recorded on the cell assembly at room temperature (298 K) in the current range 0 to 1000 mA cm^{-2}. Cell voltage vs time plots were recorded continuously, and impedance spectra were periodically acquired at OCP.

3 | RESULTS AND DISCUSSION

3.1 | Electrophoretic deposition of Co_3O_4 nanopowders

A key aspect in the application of the EPD technique is the choice of a suitable suspending medium able to charge the suspended particles and favoring their transport and coagulation at the surface of the electrode to form an uniform layer once an electric field is applied. The optimization of the deposition process requires, therefore, an accurate tailoring of the liquid phase composition.[20]

For the deposition of Co_2O_3 nanoparticles, we propose a solution of acetylacetone, iodine, and water as it has been already successfully employed in the deposition and co-deposition of several ceramic material. It was previously demonstrated that an amount of water in solution ranging from 10 to 20 mL L^{-1} can maximize the deposition rate of the process and ensure the formation of a uniform, crack free layer of particles.[19,21] After preliminary tests, we have therefore selected the composition of 10 mL L^{-1} of water and 2.5 g L^{-1} of metal iodine dissolved in acetylacetone. In order to optimize the catalytic properties of the composite electrode, our attention has so focused on the preparation of the EPD layers coated with different amounts of Co_3O_4 nanoparticles by appropriately varying three specific parameters in certain intervals:

- concentration of Co_3O_4 in suspension (0.1-3 g L^{-1}).
- deposition times (20-300 seconds).
- applied voltage (from 30 to 40 V).

Table 2 lists the samples together with the selected deposition parameters and the Co_3O_4 loads, calculated by weight difference after the solvent evaporation and before the heat treatment.

Figures 4 and 5 show the trend of the deposited Co_3O_4 as a function of the deposition time and of the Co_3O_4 in suspension, respectively. Both parameters have a strong influence on the EPD process, as the deposited Co_3O_4 increases almost linearly.

The deposit varies from a minimum of 0.025 to a maximum of 4.052 mg cm^{-2}. The deposition maximum is in line with values reported in the literature for other deposition methods such as spray coating or brushing, typically around 5 mg cm^{-2}.[9,22] After the heat treatment, no macroscopic cracks or delamination are visible (Figure 6).

The SEM analysis of the fibers, as received in the steel support, after the heat treatment, after EPD and subsequent heat treatment, at low magnification (Figure 7) clearly highlights some morphological changes. Fibers are initially smooth (diameter about 7 μm) except for the presence of small homogeneously diffused impurities. After heat treatment in air, the fibers appear uniformly coated by a thin homogeneous layer, most likely a mixed oxide of the various metals of which the steel is composed (Fe, Ni, and Cr). The situation changes radically after electrophoretic deposition and the subsequent heat treatment. A similar SS surface is decorated by well-adhered swellings of particles and agglomerates of micrometric dimensions appear.

At high-magnification SEM (Figure 8) clearly highlights the transformation undergone by the material. The originally smooth surface appears completely covered by a rough and homogeneous structure characterized by nano-scale particles and in which a certain degree of porosity is visible.

TABLE 2 Deposition parameters and Co_3O_4 weight via EPD

Sample	Co_3O_4 (susp.) g L^{-1}	Deposition time sec	Applied voltage V	Co_3O_4 (dep.) mg cm^{-2}
SS ed SS-TT	-	0	-	-
SS/EPD-Co-9	0.100	20	30	0.0250
SS/EPD-Co-10	0.200	20	30	0.0625
SS/EPD-Co-11	0.375	20	30	0.0750
SS/EPD-Co-12	0.375	40	30	0.1125
SS/EPD-Co-13	0.375	60	30	0.2250
SS/EPD-Co-14	0.375	180	30	0.5625
SS/EPD-Co-15	0.375	300	30	0.9130
SS/EPD-Co-16	3.000	240	40	4.0525
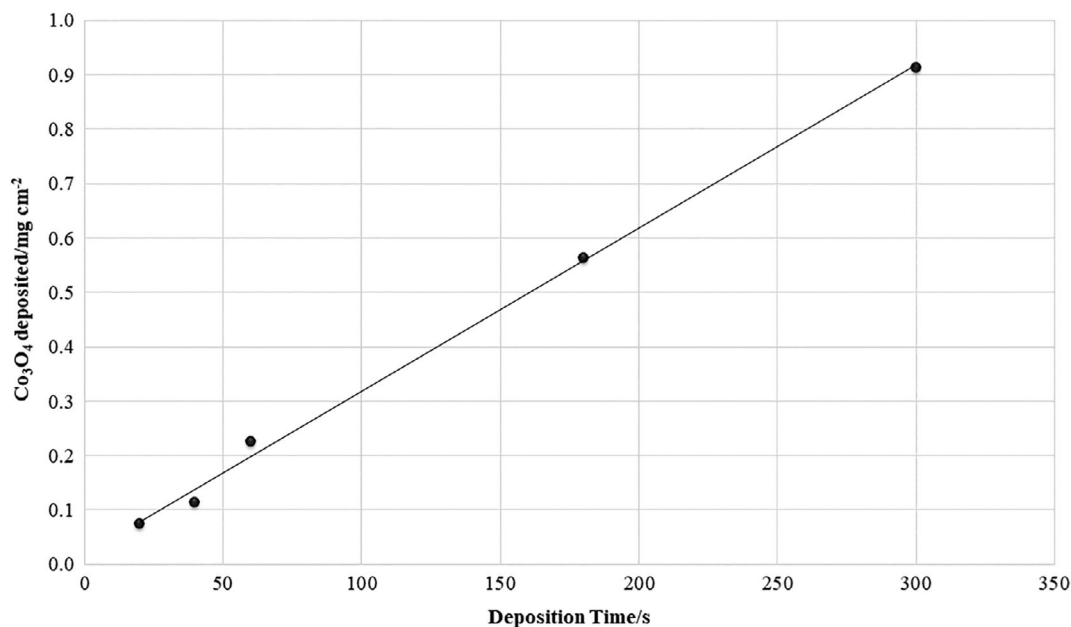
FIGURE 4 Co_3O_4 deposited via EPD as a function of deposition time at a constant voltage of 30 V and at a concentration of Co_3O_4 of 0.375 g L^{-1}

The XPS analysis of the surface on two samples (SS/EPD-Co-15 and SS/EPD-Co-16) confirms the presence of Co amount as a function of the deposited load, as evidenced by the simultaneous attenuation of the characteristic signal of iron (710 eV), the main constituent of the steel substrate and the appearance of the characteristic signal of the Co doublet (Co_3O_4) at 814 eV ($2p_{1/2}$) and 780 eV ($2p_{3/2}$). The spectra for the three samples are shown in Figures 9 and 10 for the characteristic regions of Fe2p and Co2p and have the characteristic shape of the respective oxidized forms.

The quantitative analysis of the atomic percentage of the elements obtained from the XPS data on the three samples provides the values shown in Table 3. We observe the progressive increase in Co and the decrease in the signal of Fe and Cr, "obscured" by the Co layer on the surface. The apparent progressive decrease of the O signal and its shape, not reported here, are difficult to interpret due to the important presence of contamination carbon on the surface that can also be bonded to oxygen, which does not allow unique attributions to known chemical components.

3.2 | Electrochemical characterization of SS/EPD electrodes

The electrochemical characteristics of the EPD anodes were compared to the SS supports, as received and after the high-temperature thermal treatment. Figure 11 shows the voltammetries highlighting a different behavior for the three electrodes whose maximum current density follows
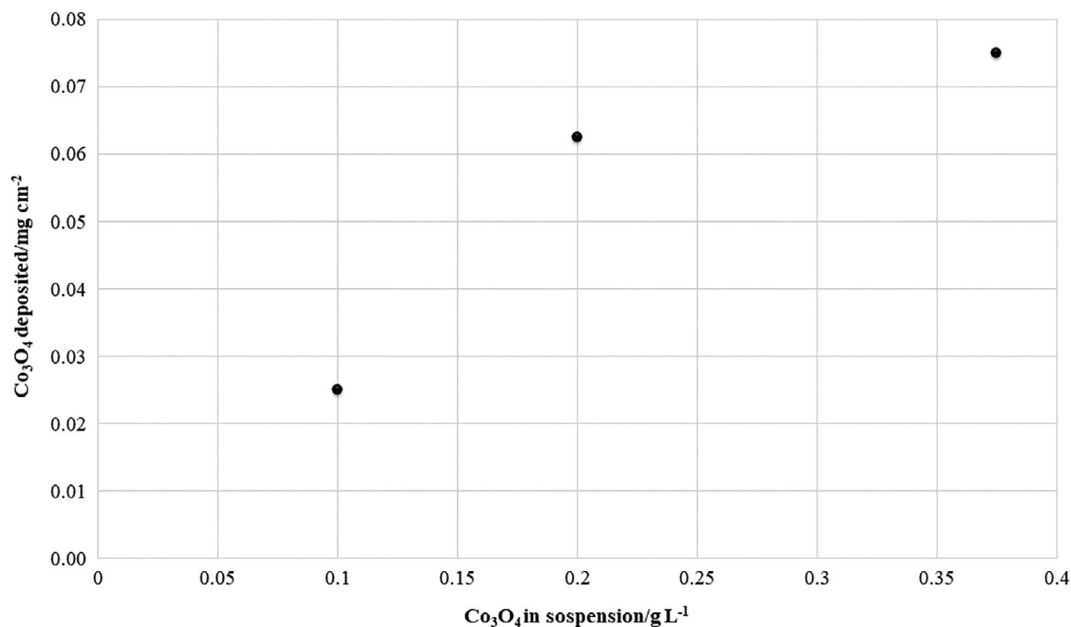
FIGURE 5 Co_3O_4 deposited via EPD as a function of the amount of Co_3O_4 in suspension at a constant voltage of 30 V

(A) **SS**

(B) **SS-TT**

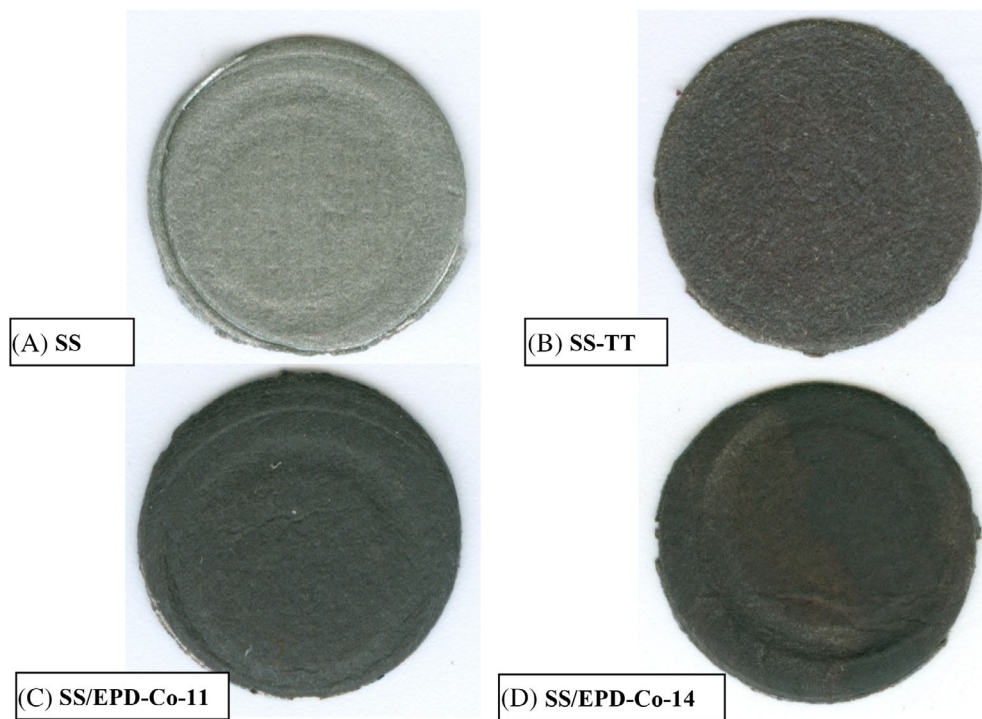(C) **SS/EPD-Co-11**

(D) **SS/EPD-Co-14**

FIGURE 6 Photographs of the substrates (area 2 cm^2) as received, A; after heat treatment, B; after coating with 0.075 mg cm^{-2}, C; and with 0.565 mg cm^{-2}, D; of a Co_3O_4 deposit and subsequent heat treatment

the trend SS/EPD-Co > SS-TT > SS. The heat treatment on the steel already produces an increase in the maximum current of about 21% at 1.75 V vs NHE; this is probably due to the formation of surface oxides of Fe and Ni with greater catalytic activity for OER.[23] The deposition of Co_3O_4 and the subsequent heat treatment further enhances the current to 46%. The onset potential for oxygen discharge shows the opposite trend, decreasing from about 1.0 V vs NHE for SS to 0.91 V for SS-TT, down to about 0.79 V for SS/EPD-Co (insert Figure 11). Recalling that the thermodynamic potential for the discharge of oxygen in an alkaline environment is approximately 0.401 V vs NHE, the electrode potential in Figure 8, up to this constant, represents the overvoltage for the OER;
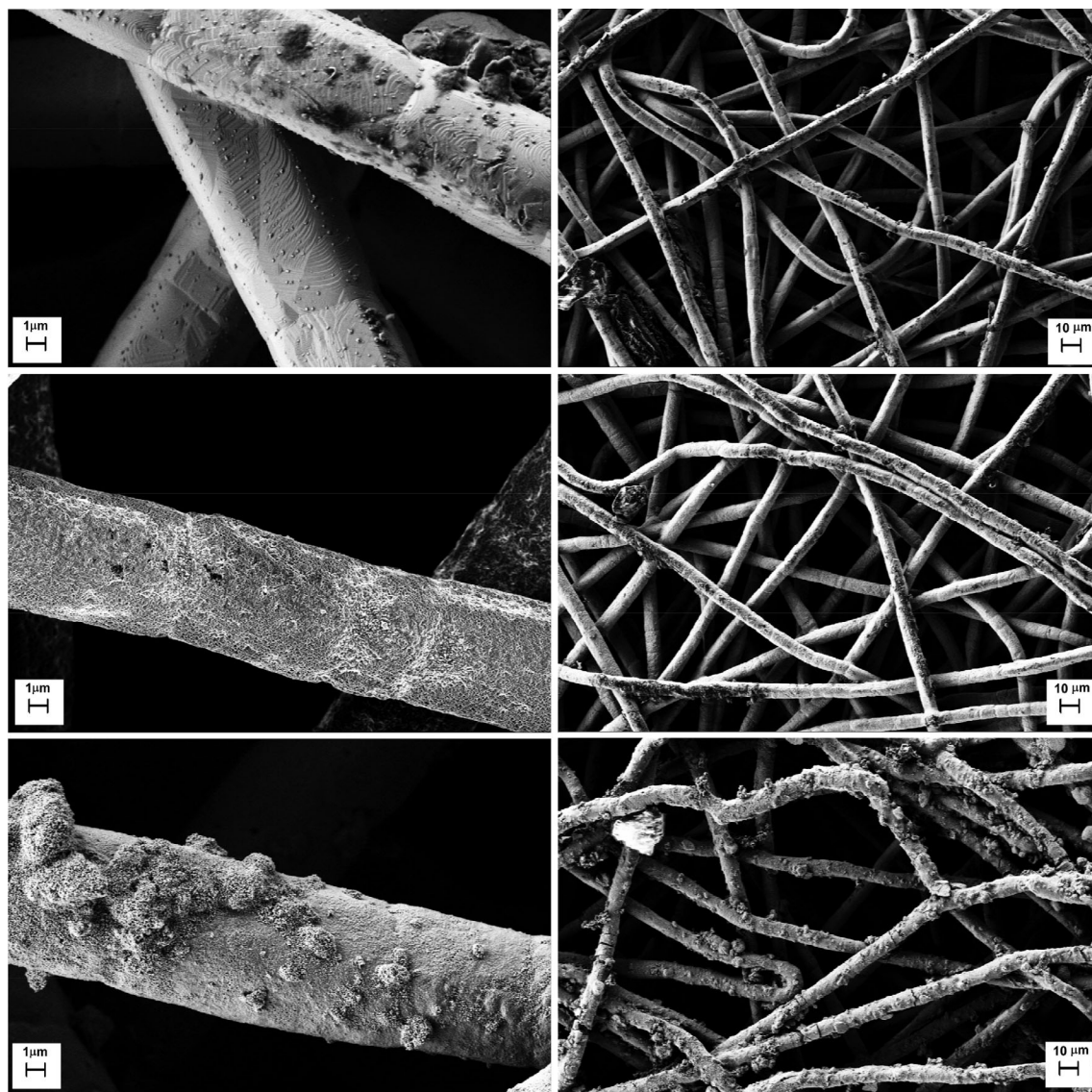
$$2OH^- \rightarrow 1/2O_2 + 2e^- + H_2O \qquad (1)$$
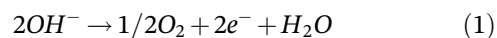
FIGURE 7 SEM photo of GDE as received (top), after heat treatment (center), and after EPD with 0.91 mg cm^{-2} (bottom) of a Co$_3$O$_4$ deposit

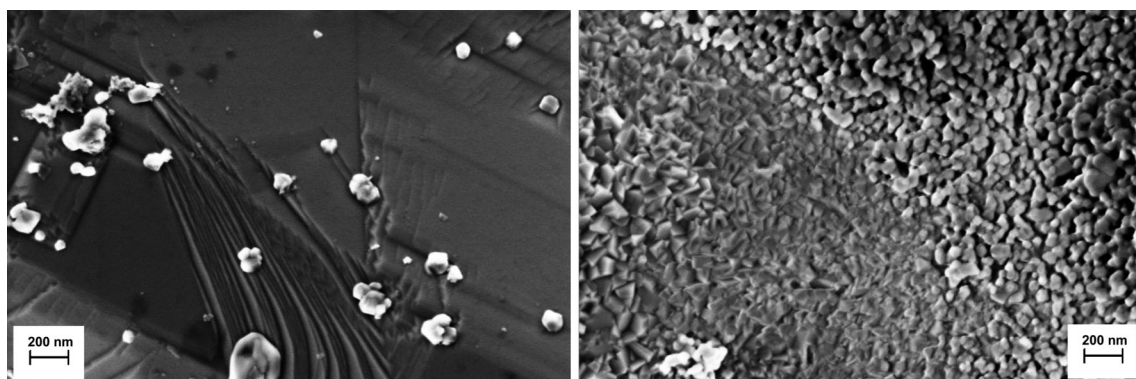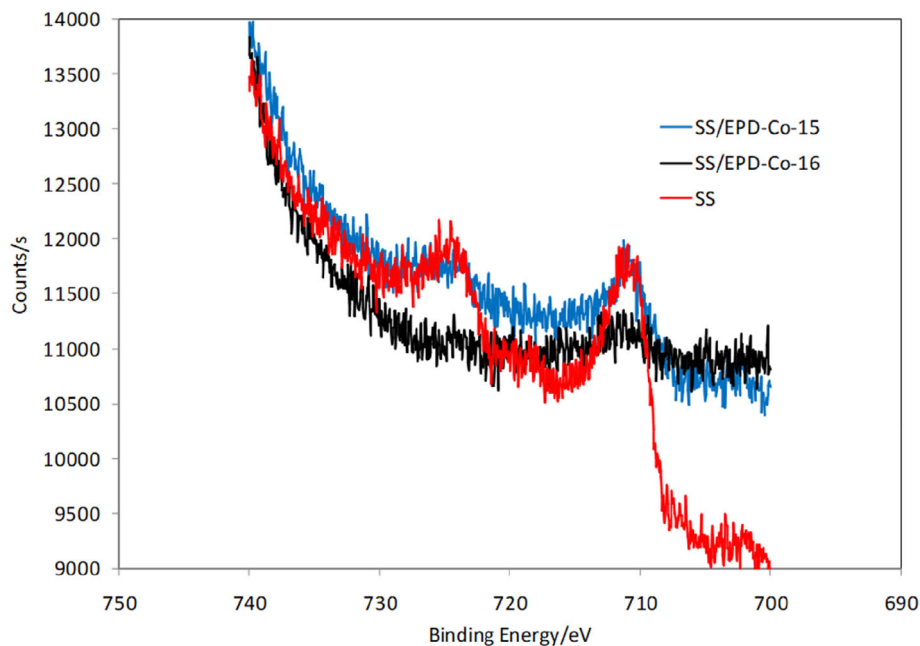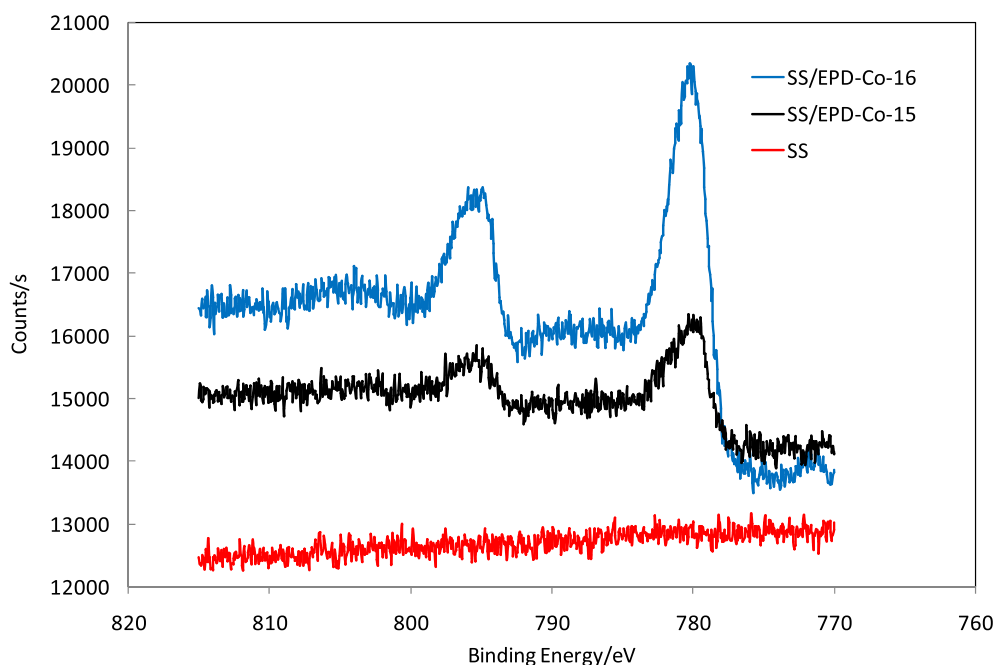**FIGURE 8** SEM photo of GDE as received (left) and after EPD with 0.91 mg cm^{-2} (right) of a Co$_3$O$_4$ deposit

FIGURE 9 XPS spectra of SS, SS/EPD-Co-15, and SSEPD-Co-16 anodes; Fe signal range

**FIGURE 10** XPS spectra of SS, SS/EPD-Co-15, and SS/EPD-Co-16 anodes; Co signal range

TABLE 3 XPS elemental composition of the analyzed samples.

Elemento	SS (at%)	SS/EPD-Co-15 (at%)	SS/EPD-Co-16 (at%)
Fe2p	12.0	4.0	2.0
Co2p	0.0	10.5	27.9
Cr2p	3.1	1.6	0.0
O1s	84.9	83.9	70.1

Therefore, the data show that the EPD method is capable to effectively increase the catalytic activity by reducing the overvoltage of almost 200 mV compared to the steel substrate.

Figure 12 shows the polarization curve of a few SS/EPD electrodes with increasing loads of cobalt oxide from 0.025 to 0.91 mg cm^{-2} compared to SS-TT. The results show that even a small amount of Co_3O_4 modifies
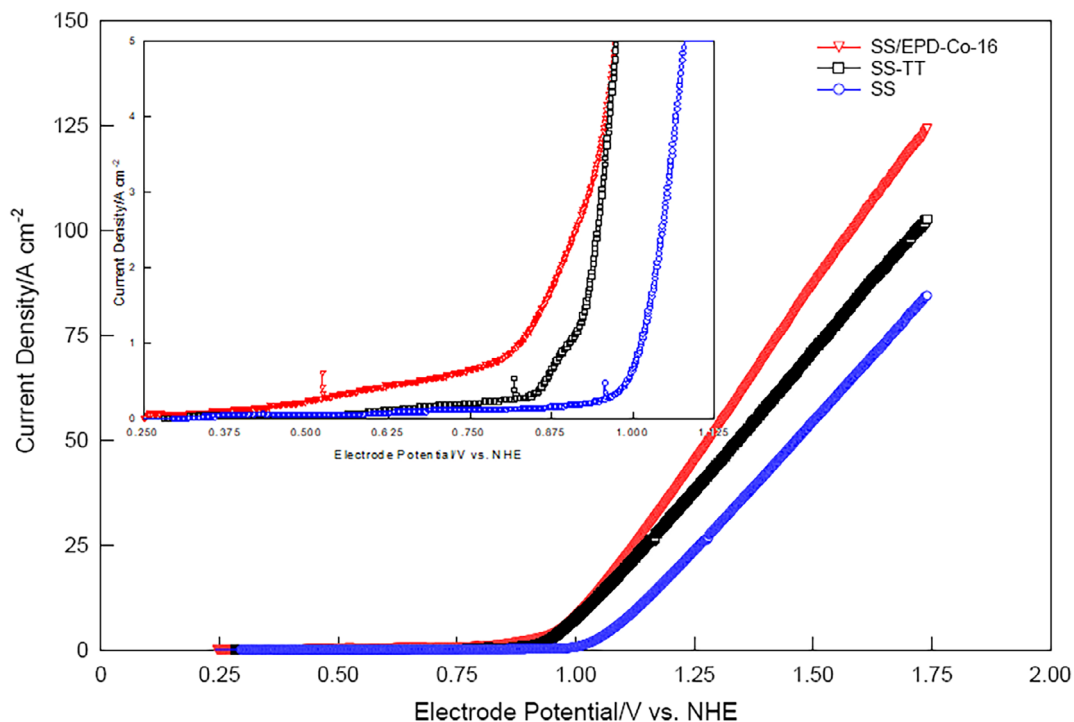
FIGURE 11 Voltammetries (1 mV s^{-1}) in 0.5 M KOH at 25°C for steel electrode before (SS) and after heat treatment at 560°C (SS-TT) compared with SS/EPD-Co-16 electrode (Co$_3$O$_4$ 4 mg cm^{-2})

FIGURE 12 Electrode potential vs current density for anodes with different Co$_3$O$_4$ load in 0.5 M KOH at 25°C
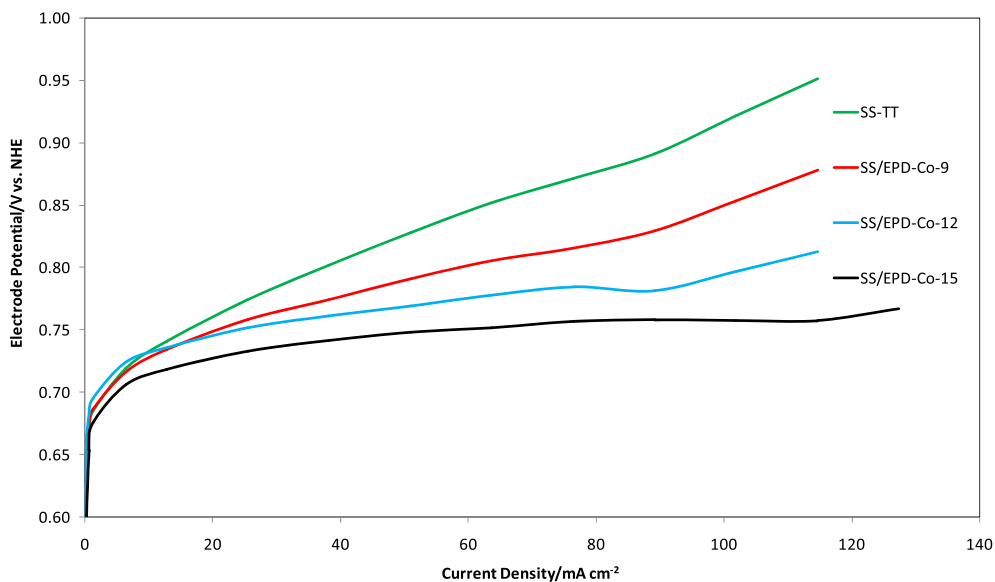
the electrochemical properties of the SS support material: it was observed that with a load of just under 1 mg cm^{-2}, the electrode potential is greatly reduced.

A further verification of the effectiveness of catalyst EPD is made evident by the comparison of SS/EPD-Co-16 with 4.0 mg cm^{-2} with electrodes made of different materials and/or produced with ED techniques: Ni72%-Co27% alloy, (Ni-Co-alloy), nickel, and nickel with electrodeposited Pt (0.75 mg cm^{-2}) (nickel/Pt).

Figure 13 shows the voltammetries performed on these different samples, highlighting the different behavior of the electrodes according to the predominant element on the surface at the catalytic level. The maximum current density follows the trend Pt > Co > Ni with Ni/Pt at approximately 170 mA cm^{-2} and the Ni at 38 mA cm^{-2}. All samples containing cobalt show an intermediate and fairly similar behavior with a maximum current of about 120 mA cm^{-2}, although the content of
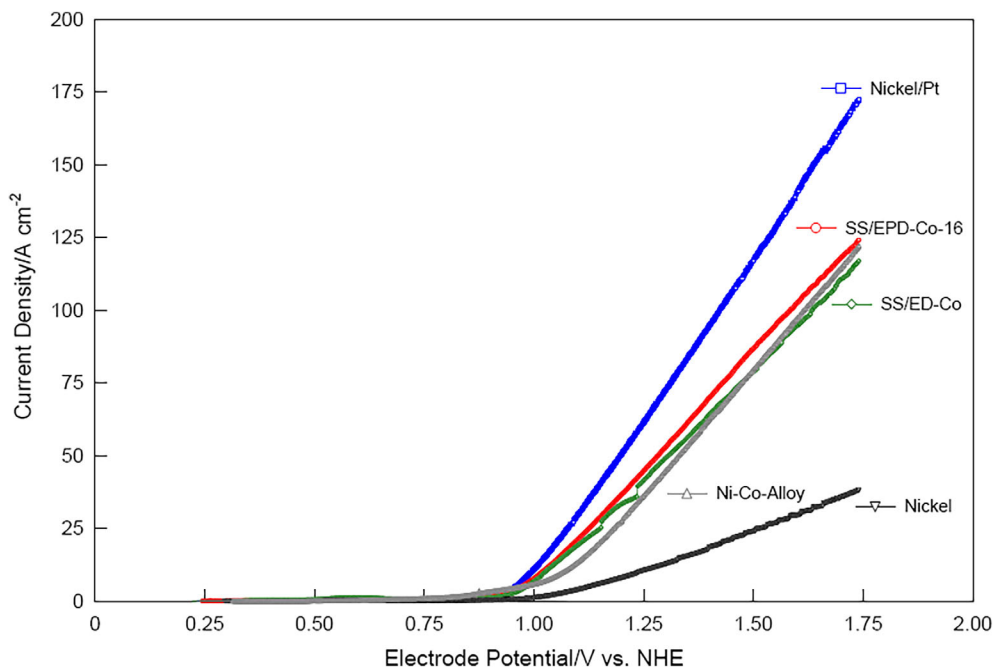
FIGURE 13 Voltammetries (1 mV s^{-1}) in 0.5 M KOH at 25°C for nickel, nickel/Pt, SS/ED-Co, Ni-Co alloy, and SS/EPD-Co-16 (Co$_3$O$_4$ 4 mg cm^{-2})
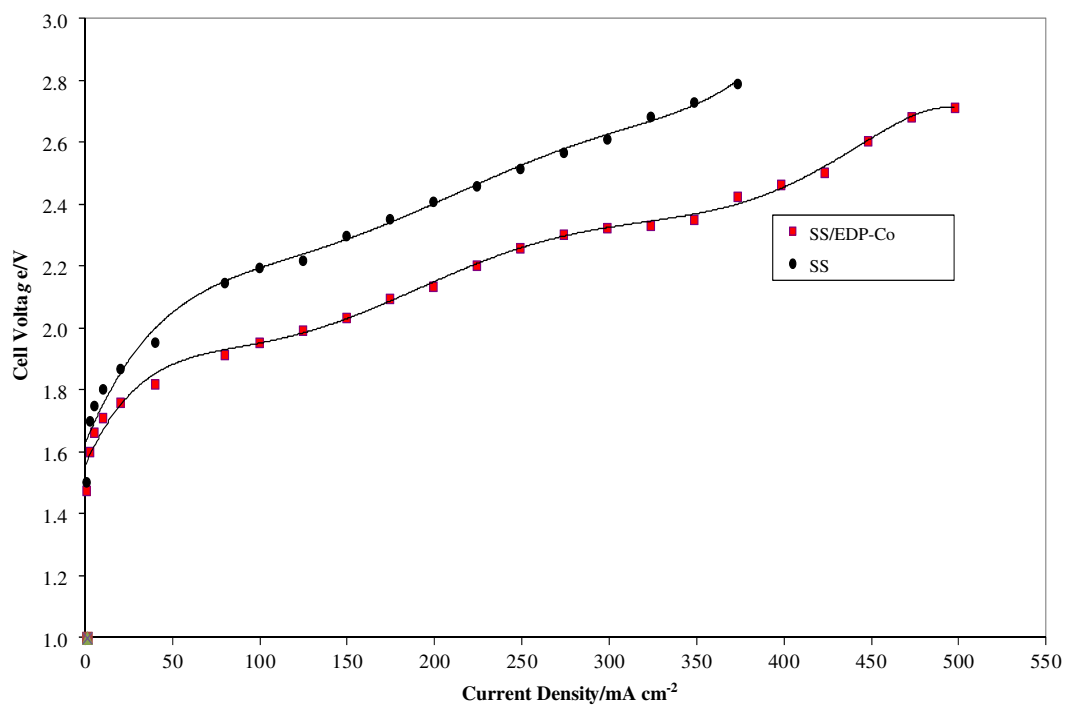

FIGURE 14 Cell voltage vs current density for electrolysis cell with SS and SS/EPD-Co anodes and Ni cathode, fed with KOH 0.5 M on the anode side at 100 mL min^{-1}. Cell temperature 25°C

this metal is quite different for the three electrodes. In particular, it can be observed that SS/EPD-Co-16 shows maximum currents comparable to Ni-Co-Alloy and SS/ED-Co despite having Co loads certainly lower by at least a factor 4 if not less.

The Figure 14 finally shows the polarization results of two electrolysis cells, with the SS and SS/EPD-Co anodes, providing direct evidence of the effect of Co$_3$O$_4$ EPD deposition in improving the cell performance of about 150 mA cm^{-2} at the highest voltage.

TABLE 4 Average cell voltage, efficiency and ASR after 100 h for cell with SS, SS/EPD-Co as anodes and wire mesh Ni cathode, fed with KOH 0.5 M on the anode side at 100 ml min^{-1} at 25 °C and 0.2 A cm^{-2}.

Anode	Cell Voltage/V	η/%	ASR/Ω cm^2
SS	2.46 ± 0.04	60.1	1.2 ± 0.2
SS/EPD-Co	2.26 ± 0.02	65.5	1.2 ± 0.2

Table 4 summarizes the average cell voltage, at 200 mA cm^{-2}, and efficiency[24] in the first 100 hours for the cell with the two different anodes, evidencing the stability of performance in the short time for all the electrodes. The trend for the voltage ($E_{SS/EPD-Co} < E_{SS}$) confirms the good performance for the cobalt oxide–modified anode. Also, the ASR was measured during time in order to verify the membrane stability and confirm that the observed difference was due only to the anodes. The cell showed a constant trend in ASR evidencing good membrane stability. In subsequent tests, it will be necessary to check the stability for longer times.

4 | CONCLUSION

In this work, a new anodic catalyst deposition methodology for alkaline membrane cells was developed. The method based on electrophoretic deposition technology allows to rapidly and reproducibly obtain cobalt oxide coatings on steel supports. In the specific case, coating with Co_3O_4 nanoparticles of the porous steel anodes considerably improves the electro-catalytic properties of the electrode as evidenced by the comparison with materials with known activity for OER. The electrophoretic deposition of anodes with cobalt oxides is therefore a reliable, fast, and safe method to produce electrodes with an extended surface, while improving their ability to work in this type of electrolyzers. This preparative technique offers several advantages, such as high deposition rate, simple apparatus, and no binder required. In the near future, the preparation of catalyst coated substrates will now be extended to the cathode side, so that complete electrolysis cells could be made by simple and cost-effective electrophoretic deposition.

ORCID
Alfonso Pozio https://orcid.org/0000-0001-8358-5160

REFERENCES
1. M. Wang, Z. Wang, X. Gong, Z. Guo, "The intensification technologies to water electrolysis for hydrogen production—a review", *Renew Sustain Energy Rev*, 29 2014, 29, 573–588.
2. Kiaee M, Infield D, Cruden A. Utilisation of alkaline electrolysers in existing distribution networks to increase the amount of integrated wind capacity. *J Energy Storage*. 2018;16:8-20.
3. Matute G, Yusta JM, Correas LC. Techno-economic modelling of water electrolysers in the range of several MW to provide grid services while generating hydrogen for different applications: a case study in Spain applied to mobility with FCEVs. *Int J Hydrogen Energy*. 2019;44:17431-17442.
4. Chisholm G, Cronin L. Chapter 16—hydrogen from water electrolysis. *Storing Energy*. 2016:315-353. http://dx.doi.org/10.1016/B978-0-12-803440-8.00016-6
5. Colli AN, Girault HH, Battistel A. Non-precious electrodes for practical alkaline water electrolysis. *Materials*. 2019;12:1336-1353.
6. Perez-Alonso FJ, Adan C, Rojas S, Pena MA, Fierro JLG. Ni/Fe electrodes prepared by electrodeposition method over different substrates for oxygen evolution reaction in alkaline medium. *Int J Hydrogen Energy*. 2014;39:5204-5212.
7. Roy A, Watson S, Infield D. Comparison of electrical energy efficiency of atmospheric and high-pressure electrolysers. *Int J Hydrogen Energy*. 2006;31:1964-1979.
8. Leng Y, Chen G, Mendoza AJ, Tighe TB, Hickner MA, Wang CY. Solid-state water electrolysis with an alkaline membrane. *J Am Chem Soc*. 2012;134:9054-9057.
9. Vincent I, Bessarabov D. Low cost hydrogen production by anion exchange membrane electrolysis: a review. *Renew Sustain Energy Rev*. 2018;81:1690-1704.
10. Marini S, Salvi P, Nelli P, et al. Advanced alkaline water electrolysis. *Electrochim Acta*. 2012;82:384-391.
11. J. Hnát, M. Plevova, R.A. Tufa, J. Zitka, M. Paidar, K. Bouzek, "Development and testing of a novel catalyst-coated membrane with platinum-free catalysts for alkaline water electrolysis". *Int J Hydrogen Energy*, 2019;44(33):17493–17504.
12. Kjartansdottir CK, Nielsen LP, Møller P. Development of durable and efficient electrodes for large-scale alkaline water electrolysis. *Int J Hydrogen Energy*. 2013;38:8221-8231.

13. Pozio A, Lisi N, Della Seta L, Dolci S, D'Angelo C. Effect of cobalt deposition on Ni anodes for alkaline membrane water electrolyser. *Mater Chem Phys*. 2020;242:122537.

14. Wu MS, Huang CY, Lin KH. Electrophoretic deposition of nickel oxide electrode for high-rate electrochemical capacitors. *J Power Sources*. 2009;186:557-564.

15. Hu S, Li W, Finklea H, Liu X. A review of electrophoretic deposition of metal oxides and its application in solid oxide fuel cells. *Adv Colloid Interface Sci*. 2020;276:102102.

16. A.R Boccaccini, I. Zhitomirsky, "Application of electrophoretic and electrolytic deposition techniques in ceramics processing", *Curr Opin Solid State Mater Sci*, 2002;6(3):251-260.

17. I. Zhitomirsky, Adv. "Cathodic electrodeposition of ceramic and organoceramic materials. Fundamental aspects". *Colloid Interface Sci* 2002, 97/29, 279-317.

18. Gurrappa I, Binder L. Electrodeposition of nanostructured coatings and their characterization—a review. *Sci Technol Adv Mater*. 2008;9:043001-043012.

19. Bozza F, Schafbauer W, Meulenberg WA, Bonanos N. Characterization of $La_{0.995}Ca_{0.005}NbO_4$/Ni anode functional layer by electrophoretic deposition in a $La_{0.995}Ca_{0.005}NbO_4$ electrolyte based PCFC. *Int J Hydrogen Energy*. 2012;37:8027-8032.

20. F. Bozza, R. Polini, E. Traversa, "Electrophoretic deposition of dense Sr- and mg-doped $LaGaO_3$ electrolyte films on porous La-doped ceria for intermediate temperature solid oxide fuel cells", *Fuel Cells*, 2008;8(5):344-350.

21. Glasscock JA, Mikkelsen L, Persson AH, et al. Porous Fe21Cr7Al1Mo0.5Y metal supports for oxygen transport membranes: Thermo-mechanical properties, sintering and corrosion behavior. *Solid State Ion*. 2013;242:33-44.

22. Faid AY, Barnett A, Seland F, Sunde S. Highly active nickel-based catalyst for hydrogen 3 evolution in anion exchange membrane electrolysis. *Catalyst*. 2018;8:614-627.

23. Cossar E, Barnett AO, Seland F, Baranova EA. The performance of nickel and nickel-iron catalysts evaluated as anodes in anion exchange membrane water electrolysis. *Catalysts*. 2019;9:814-830.

24. Phillips R, Dunnill CW. Zero gap alkaline electrolysis cell design for renewable energy storage as hydrogen gas. *RSCAdv*. 2016;6:100643-100651.